

C₂₀, the Smallest Fullerene

Fei Lin

University of Illinois
at Urbana-Champaign

Erik S. Sørensen

McMaster University

Catherine Kallin

McMaster University

A. John Berlinsky

McMaster University

29.1 Introduction	29-1
29.2 Molecular Structure	29-2
29.3 Single Molecular Properties.....	29-3
Ground State Energy • Thermal Stability • Mechanical Stability • Electron Affinity • Electron Correlation • Vibration Frequencies and Electron-Phonon Coupling	
29.4 Solid Properties.....	29-6
Superconductivity? • <i>I-V</i> Characteristics of Cage Chains	
29.5 Summary and Future Perspective.....	29-9
Acknowledgments.....	29-9
References.....	29-9

29.1 Introduction

The C₂₀ molecule with a dodecahedral cage structure is the smallest member of the fullerene family. It follows from Euler's theorem that fullerenes are molecules that consist of exactly 12 pentagons and a varying number of hexagons. The most famous fullerene molecule is C₆₀ with 12 pentagons and 20 hexagons (commonly referred to as "Buckyballs," short for "Buckminsterfullerene"), which was discovered in 1985 (Kroto et al. 1985). Smalley, Curl, and Kroto were awarded the 1996 Nobel Prize in Chemistry for their discovery, which not only allowed the study of the fascinating properties of C₆₀ molecules and solids, such as superconductivity in alkali-metal-doped C₆₀ solid (Hebard et al. 1991), but also initiated an exciting new era of carbon nanotechnology. Interestingly, in his Nobel lecture, Kroto (1997) emphasizes the *pentagon isolation rule* (Kroto 1987, Schmalz et al. 1988) predicting the most stable fullerenes to have the 12 pentagons as far apart as possible. In light of this rule, the C₂₀ fullerene cage should be highly unstable, and by defying this rule C₂₀ is sometimes referred to as an "unconventional fullerene" (Xie et al. 2004, Wang et al. 2006).

Not surprisingly, the synthesis of the smallest fullerene is therefore much more difficult than that of C₆₀, since the highly curved fullerene C₂₀ is so reactive that it cannot be produced by carbon condensation or cluster annealing processes. Instead, Prinzbach et al. (2000) started from a precursor [dodecahedrane C₂₀H₂₀, which was first synthesized by the Paquette group (Ternansky et al. 1982, Paquette et al. 1983)]. They replaced the hydrogen atoms with bromine atoms, and then debrominated to produce the gas-phase cage C₂₀ fullerene. The same process is used to synthesize another C₂₀ isomer with a bowl molecular structure. These two isomers, together with the previously

commonly produced monocyclic ring, constitute the three major isomers of C₂₀ that are of particular interest for this chapter.

It is worth noting that the C₂₀ cage isomer has been the subject of intensive theoretical research even before its production in 2000. A vast amount of theoretical work has used density functional theory (DFT) to study the relative stability of cage C₂₀ compared with other isomers but has arrived at no consensus. This, in part, reflects the importance of electron correlations not included in the mean-field DFT calculations. More accurate treatments of electron correlations in these molecules by quantum Monte Carlo (QMC) calculations show that the bowl isomer has the lowest energy, with the ring isomer in the middle, and with the cage isomer being highest in ground state energy (Grossman et al. 1995). This was the first QMC calculation applied to C₂₀ molecules, indicating the importance of electron correlations in determining the electronic properties of these molecules. To further explore the electronic correlations in C₂₀ molecules, Lin et al. performed exact diagonalization (ED) and QMC simulations on a one-band Hubbard model (Lin et al. 2007) using the effective Hamiltonian approach (Lin and Sørensen 2008). They found that the cage isomer is the most correlated molecule among the isomers, with an on-site interaction and hopping integral ratio as high as $U/t \sim 7.1$.

Two research groups (Wang et al. 2001, Iqbal et al. 2003) have recently reported the synthesis of solid C₂₀ phases. Wang et al. used ion beam irradiation to produce a close-packed hexagonal crystal consisting of C₂₀H₂₀ molecules with a lattice spacing of 4.6 Å. Iqbal et al. employed ultraviolet laser ablation from diamond onto nickel substrates and obtained a face-centered-cubic (fcc) lattice with 22 carbon atoms per unit cell (C₂₀ linked with bridging carbon atoms at interstitial tetrahedral sites). These

further developments are likely to stimulate more research interest in this field, since speculation (Miyamoto and Saito 2001, Spagnolatti et al. 2002) about a possible superconducting state in the C_{20} solid can now be tested experimentally. Interest in a possible superconducting state of solid C_{20} is a natural outgrowth of the superconductivity observed in doped C_{60} that has an fcc lattice structure. A higher transition temperature, T_c , might be expected for solid C_{20} than for C_{60} because the more curved molecular structure of the C_{20} cage implies a higher frequency vibrational phonon. Of course, the expectation of this higher T_c is based on the phonon mechanism for superconductivity, while the question of whether phonons or electron–electron interactions are responsible for the superconducting behavior in the doped C_{60} solid is still a subject of debate.

We organize this chapter in the following way. We first describe the molecular structure of C_{20} fullerene. This is followed by a discussion of various single molecular properties, including ground state energy, thermal stability, mechanical stability, electron affinity, electron correlations, vibrational frequencies, and electron–phonon coupling strength. We then proceed to discuss the electronic properties of the solid C_{20} fullerene, possible superconductivity, and the I – V characteristics of short chains of fullerene C_{20} . The chapter concludes with a future perspective.

29.2 Molecular Structure

We show in Figure 29.1 the molecular structures of the three major isomers: cage, bowl, and ring. The 20 carbon atoms in the cage form 12 pentagons and 30 bonds. This is the consequence of

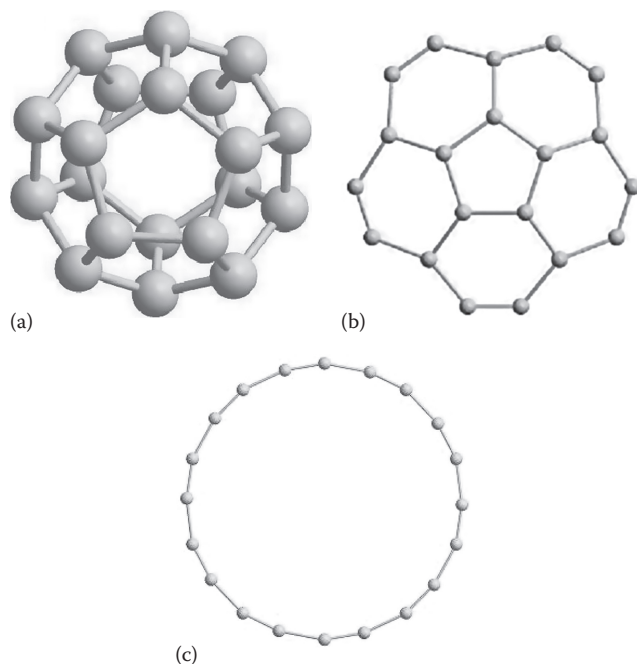


FIGURE 29.1 Molecular structures of C_{20} isomers: (a) cage, (b) bowl, and (c) ring.

Euler's formula, which relates the number of vertices, edges, and faces on a polygon, i.e., $V - E + F = 2$. The molecular diameter is about 3.1 Å. The fullerene cage C_{20} has the molecular symmetry of the icosahedral point group I_h , which has 120 symmetry operations. It is the only fullerene smaller than C_{60} with the full I_h symmetry. The I_h group is discussed by Ellzey (2003), Ellzey and Villagran (2003), and Ellzey (2007), and the application of this symmetry to the Hückel Hamiltonian defined on a cage results in the symmetry-labeled Hückel energy diagram shown in Figure 29.2. The Hückel Hamiltonian, in second quantization notation, can be written as

$$H = -t \sum_{\langle ij \rangle \sigma} (c_{i\sigma}^\dagger c_{j\sigma} + \text{h.c.}), \quad (29.1)$$

where

t is the nearest neighbor (NN) hopping integral that sets the energy scale of the system

$c_{i\sigma}^\dagger (c_{i\sigma})$ creates (annihilates) an electron with spin σ on the i th carbon site

h.c. is the Hermitian conjugate

$\langle ij \rangle$ means i and j are NN

The above noninteracting Hückel Hamiltonian will be regarded as an effective Hamiltonian that captures the geometric character of the cage molecule. It is an approximation to the real Hamiltonian, and should have a low-energy spectrum around the Fermi energy very similar to that of the real Hamiltonian. One can obtain a value for the hopping integral, t , by fitting the tight-binding Hückel energy levels around the Fermi level to those from DFT calculations (Lin and Sørensen 2008), leading to $t \approx 1.36$ eV.

From Figure 29.2, one can see that the neutral cage isomer is metallic (since the conduction bands are half-filled) and magnetic (if Hund's rule is applied to the two electrons in the highest occupied levels). Are these properties realized in a real molecule? Can they survive the inclusion of electron–electron

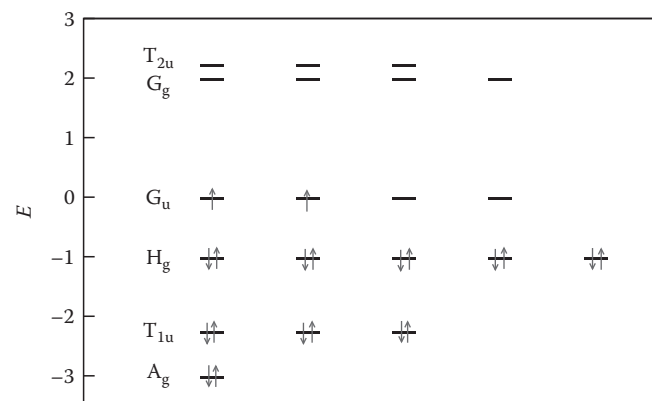


FIGURE 29.2 Hückel molecular orbitals of a neutral dodecahedral C_{20} molecule.

interactions? We will examine these questions, going beyond the noninteracting Hückel Hamiltonian, in later sections.

29.3 Single Molecular Properties

29.3.1 Ground State Energy

There are many calculations on C₂₀ isomers that compare their ground state energies and infer their relative stability. However, different ground state energy orderings are predicted by different calculations, depending on the method used. Hartree–Fock (HF) calculations show that the ring is lowest in energy, followed by the bowl and then the cage (Parasuk and Almlöf 1991, Feyereisen et al. 1992). Local density approximation (LDA) calculations predict the cage to be the lowest in energy, followed by the bowl and the ring (Brabec et al. 1992, Wang et al. 1996). Generalized gradient approximation (GGA) (Raghavachari et al. 1993), hybrid HF/DFT (Allison and Beran 2004), and DFT/B3LYP (Xu et al. 2006) suggest again the same ground state energy ordering as HF calculations. The more accurate coupled-cluster calculations (CCSD) with basis set including single, double, and triple excitations of the HF wave-function gives an energy ordering similar to LDA, i.e., the cage and the bowl are almost degenerate and have lower energy than the ring isomer (Taylor et al. 1995). More recent CCSD calculations are able to distinguish the energy difference between the bowl and the cage, and identify the bowl energy as lower than the cage (An et al. 2005). Tight-binding calculations based on the Harrison scheme (Harrison 1989) give the cage as the lowest energy isomer, followed by the bowl and the ring (Cao 2001). Though inconclusive, all these calculations do reflect the subtlety in making approximations about electronic correlations. The need for an accurate method, such as QMC, to deal with such correlations is clear. Such a QMC calculation with a pseudopotential replacing the ion core has been performed (Grossman et al. 1995), and gives a ground state energy ordering with the bowl being the lowest, followed by the ring and the cage. Even more accurate all-electron

(without pseudopotential) QMC (Sokolova et al. 2000) has also been done and gives the same result as Grossman et al. (1995). Therefore, one can now conclude that the ground state energy of the three major C₂₀ isomers with respect to bowl, from lowest to highest, are bowl (0 eV), ring (1.1 ± 0.5 eV), and cage (2.1 ± 0.5 eV) (Grossman et al. 1995, Sokolova et al. 2000).

We summarize the above discussion in Table 29.1.

29.3.2 Thermal Stability

From the previous discussion, we conclude that the bowl has the lowest ground state energy, and the cage has a relative energy of about 2.1 eV with respect to the bowl. Then why does the cage exist after it is produced and not decay into the lower energy isomers? Tight-binding molecular-dynamics (TBMD) simulations (Davydov et al. 2005) have helped answer this question. In the simulation, one starts with the cage isomer, and measures how many saddle point states (local energy maximum) and metastable states (local energy minimum) need to be passed over before reaching the bowl isomer state. By this process, the minimum potential barrier that must be overcome for a cage decay is measured to be about 5.0 eV. And remarkably, although many routes can be taken in the cage decay to some metastable states, none of these metastable states lead to a transition to the bowl configuration (which is the global energy minimum). This same cage stability is also found when the activation energy, E_a , for cage isomer decay is measured. The activation energy is defined as

$$N_c = N_0 \exp\left(\frac{E_a}{k_B T}\right), \quad (29.2)$$

where N_c is the critical number of steps of TBMD simulations, and $N_c = \tau/t_0$ with τ the lifetime of the cage isomer and $t_0 = 2.72 \times 10^{-16}$ s the time step of TBMD. By simulating the decay process at different temperatures, one can map out the $\ln(N_c)$ vs $1/T$ curve,

TABLE 29.1 Ground State Energy Ordering for Three C₂₀ Major Isomers from Various Calculations

Source	Method	Ground State Energy Ordering
Parasuk and Almlöf (1991)	HF	$E_{\text{ring}} < E_{\text{bowl}} < E_{\text{cage}}$
Feyereisen et al. (1992)	HF	$E_{\text{ring}} < E_{\text{bowl}} < E_{\text{cage}}$
Brabec et al. (1992)	LDA	$E_{\text{cage}} < E_{\text{bowl}} < E_{\text{ring}}$
Wang et al. (1996)	LDA	$E_{\text{cage}} < E_{\text{bowl}} < E_{\text{ring}}$
Raghavachari et al. (1993)	GGA	$E_{\text{ring}} < E_{\text{bowl}} < E_{\text{cage}}$
Allison and Beran (2004)	Hybrid HF/DFT	$E_{\text{ring}} < E_{\text{bowl}} < E_{\text{cage}}$
Xu et al. (2006)	DFT/B3LYP	$E_{\text{ring}} < E_{\text{bowl}} < E_{\text{cage}}$
Taylor et al. (1995)	CCSD	$E_{\text{cage}} \approx E_{\text{bowl}} < E_{\text{ring}}$
An et al. (2005)	CCSD	$E_{\text{bowl}} < E_{\text{cage}} < E_{\text{ring}}$
Cao (2001)	Tight-binding	$E_{\text{cage}} < E_{\text{bowl}} < E_{\text{ring}}$
Grossman et al. (1995)	QMC (pseudopotential)	$E_{\text{bowl}} < E_{\text{ring}} < E_{\text{cage}}$
Sokolova et al. (2000)	QMC (all-electron)	$E_{\text{bowl}} < E_{\text{ring}} < E_{\text{cage}}$

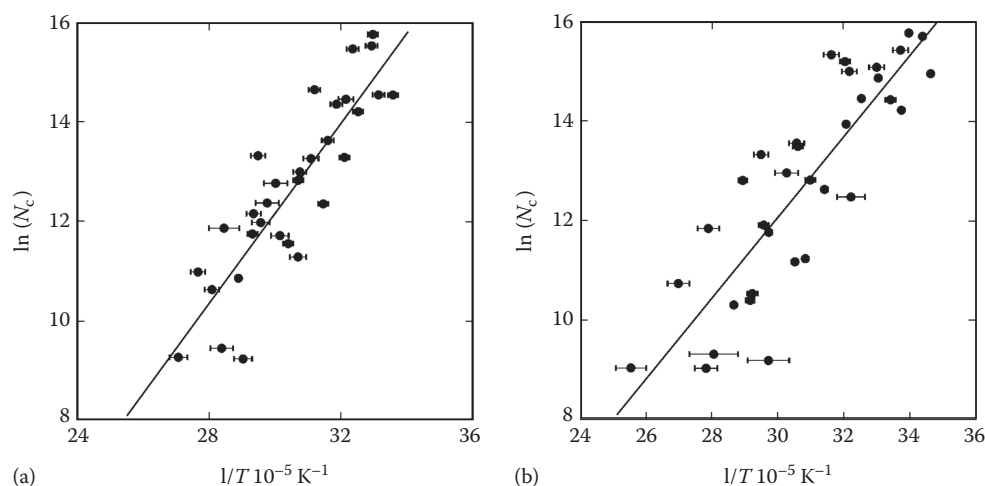


FIGURE 29.3 Logarithm of the critical number of steps of molecular-dynamics simulation, N_c , for the onset of the decay of the C_{20} fullerene as a function of the temperature, T , of the ionic subsystem for the electron temperature (a) $T_{el} = T$ and (b) $T_{el} = 0$. Circles are the results of calculation, and the solid line is a linear least square fit. (Reprinted from Davydov, I.V. et al., *Phys. Solid State*, 47, 778, 2005. With permission.)

see Figure 29.3. The slope of the fitted line gives the activation energy, $E_a = 7 \pm 1$ eV. With this activation energy, one can estimate the lifetime of the cage isomer at room temperature, τ (300 K), to be extremely large (practically infinite). This explains the stability of the fullerene cage, once it is synthesized.

There are earlier quantum molecular dynamics (QMD) studies of the free energy vs. temperature dependence for C_{20} isomers (Brabec et al. 1992), which, as we discussed in the previous section, starts from the incorrect LDA ground state energy ordering, i.e., $E_{cage} < E_{bowl} < E_{ring}$. However, these studies did see the stability of cage fullerene for temperatures below about 700 K. Above this temperature, cage fullerene transforms into its bowl isomer, which is assumed to be the building block of the C_{60} fullerene. Their conclusion is probably correct, too, since they are aiming at explaining the high-temperature production of C_{60} fullerenes in experiments using the laser vaporization technique, which we know is unable to produce C_{20} fullerene.

With the previous conclusion that the cage fullerene will not transform into other isomers once it is synthesized, it is also interesting to study further its thermal stability in the sense of the Lindemann criterion for solid melting (Lindemann 1910): solid melts when the root-mean-square bond-length fluctuation ratio, δ , exceeds a threshold value 0.1, the Lindemann constant. A QMD simulation employing the Lindemann criterion has been performed (Ke et al. 1999). Figure 29.4 shows that the C_{20} fullerenes remains solid below temperature 1900 K, above which it starts to melt.

29.3.3 Mechanical Stability

The mechanical stability of C_{20} has been studied with MD in the context of low-energy cluster beam deposition of C_{20} fullerenes on substrates (Du et al. 2002). The simulation shows that for a C_{20} kinetic energy in the range of 10–45 eV, the probability of C_{20} adsorption on the substrate is high, and the molecules maintain their dodecahedral geometry without deformation. Similar MD simulations of the mechanical stability of the C_{20} fullerene

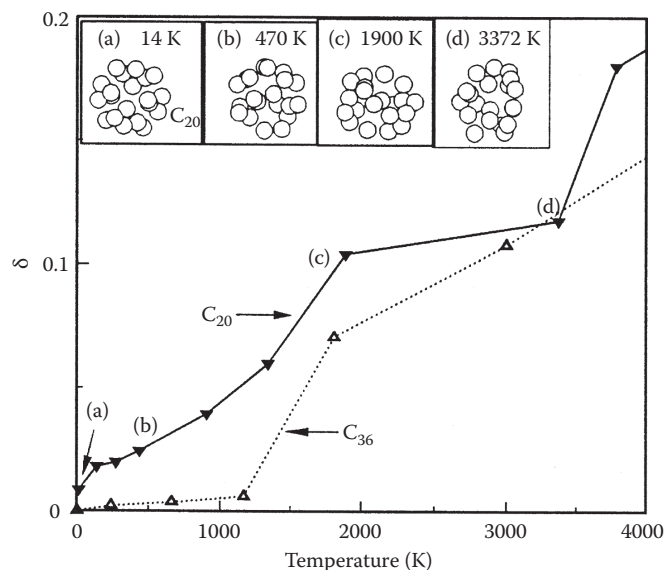


FIGURE 29.4 Root-mean-square bond-length fluctuations δ of C_{20} as a function of temperature. Snapshots (a–d) exhibit the geometry of a C_{20} cluster at various temperatures (14, 470, 1900 and 3370 K, respectively). (Reprinted from Ke, X.Z. et al., *Chem. Phys. Lett.*, 313, 40, 1999. With permission.)

AQ2

(Ke et al. 1999) also show that when the C_{20} incident energy is less than 25 eV, it will rebound without breaking after its collision with a graphite surface. These simulations are important for understanding the experimental deposition of C_{20} films.

29.3.4 Electron Affinity

Electron affinity (EA) is an important molecular property that incorporates electron correlation information (Barnett et al. 1986) and which can be measured by gas-phase photoemission experiments. EA, in the case of neutral C_{20} , is defined as

$$EA = E(20) - E(21), \quad (29.3)$$

where $E(20)$ and $E(21)$ are the internal energies of the neutral and one-electron-doped molecules, respectively. In recent years, with the development of experimental techniques, EA can be measured more and more accurately. One such example is the measurement of EA of the neutral C₂₀ molecule (Yang et al. 1987, Wang et al. 1991, Wang et al. 1999), yielding 2.7 ± 0.1 eV, 2.65 ± 0.05 eV, and 2.689 ± 0.008 eV, with increasing accuracy. Such measurements are useful for electron correlation studies and can be used to estimate the on-site electron correlation strength, as was done by Lin and Sørensen (2008), where their estimates are based on the neutral C₂₀ EA values ($EA = 2.25 \pm 0.03$ eV) measured when the gas-phase C₂₀ cage is synthesized (Prinzbach et al. 2000). Estimates of on-site electron correlation strength is the first step in the effective Hamiltonian plus QMC approach to studying molecular electronic properties.

The positive EA can also be used to understand the aggregation property of C₂₀ fullerenes (Luo et al. 2004), since it is energetically favorable for a neutral C₂₀ fullerene to obtain an additional electron to lower its energy. Without doping, such additional electrons can only be obtained by a covalent-like sharing with other fullerenes, suggesting that C₂₀ fullerenes tend to aggregate. Indeed, such aggregation phenomena have been observed not only in C₂₀ fullerenes (Ehlich et al. 2001), but also in larger fullerenes, such as C₃₆ (Piskoti et al. 1998, Collins et al. 1999), C₆₀, etc., and carbon nanotubes.

29.3.5 Electron Correlation

29.3.5.1 Beyond Noninteracting Hückel Hamiltonian

The noninteracting Hückel Hamiltonian defined in Equation 29.1 results in the electronic configuration of molecular orbitals shown in Figure 29.2. However, neglecting electron interactions is not appropriate for real materials. A more refined and minimal interacting model that takes into account electronic on-site interactions (here “sites” refers to individual C atoms) is the one-band Hubbard model defined as

$$H = -t \sum_{\langle ij \rangle \sigma} (c_{i\sigma}^\dagger c_{j\sigma} + h.c.) + U \sum_i n_{i\uparrow} n_{i\downarrow}, \quad (29.4)$$

where the additional term U represents the interaction energy of two electrons occupying the same atomic site. The ratio U/t measures the on-site interaction strength. This model has also been treated within the lattice-density functional approach (López-Sandoval and Pastor 2006). Interactions longer ranged than the on-site U has also been considered (Lin et al. 2007). Clearly, one needs first to determine how large U/t is in the real C₂₀ cage in order to address its effect on the C₂₀ electronic structure. U/t values for C₂₀ isomers have been estimated by Lin and Sørensen (2008), who show that the C₂₀ fullerene cage is the most strongly correlated of the three major C₂₀ isomers, with the on-site interaction strength as high as $U/t \sim 7.1$. The C₂₀ fullerene cage is also

the most strongly correlated molecule in the fullerene family, and is much more correlated than the C₆₀ molecule, which has a U/t ratio of approximately $U/t \sim 3.5$.

29.3.5.2 Magnetic Properties

ED and QMC calculations on Equation 29.4 have shown that, for $U/t < 4.1$, the C₂₀ fullerene has a spin triplet ground state, and for $U/t > 4.1$ it has a singlet ground state (Lin et al. 2007). Therefore, for a real neutral C₂₀ fullerene, the ground state is probably a spin singlet, violating Hund’s rule for the electron configuration of the noninteracting approach, which would predict that the neutral molecule has a spin triplet ground state (Figure 29.2). This Hund’s rule violation is a result of strong electronic correlations.

In the large U/t limit, the Hubbard model in Equation 29.4 is reduced to an antiferromagnetic Heisenberg model (AFM) using second order perturbation theory. Since $U/t \sim 7.1$, such a reduction is reasonable for the C₂₀ cage. AFM defined on a dodecahedron molecule has been solved by ED and shows a spin singlet and non-magnetic ground state (Konstantinidis 2005), which agrees very well with our previous discussions. By applying an external magnetic field, the molecule shows some interesting properties, such as magnetization discontinuities, etc. (Konstantinidis 2005, Konstantinidis 2007).

29.3.5.3 Pair-Binding Energy

The pair-binding energy as a function of on-site electron interaction has also been investigated (Lin et al. 2007) in the hope of finding a possible effective attraction between electrons on the same fullerene. The pair-binding energy is defined as

$$\Delta_b(21) = E(22) + E(20) - 2E(21), \quad (29.5)$$

as shown schematically in Figure 29.5. If $\Delta_b(21) < 0$, i.e., the non-uniform charge distribution is preferred, it would then provide an electronic mechanism for superconductivity in the alkali-doped C₆₀ materials (Chakravarty et al. 1991).

The pair-binding energy as a function of electron correlation, U/t , is shown in Figure 29.6. ED and QMC calculations show that $\Delta_b(21)$ is always positive for any value of U/t . Thus, for an average of one electron doping in the C₂₀ fullerenes, two doped electrons on two C₂₀ fullerenes tend to stay separately on two molecules instead of staying together on the same molecule and leaving the other molecule undoped. This, therefore, rules out the possibility of superconductivity from purely electronic correlations.

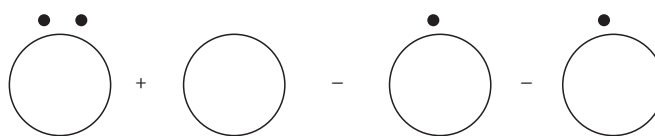
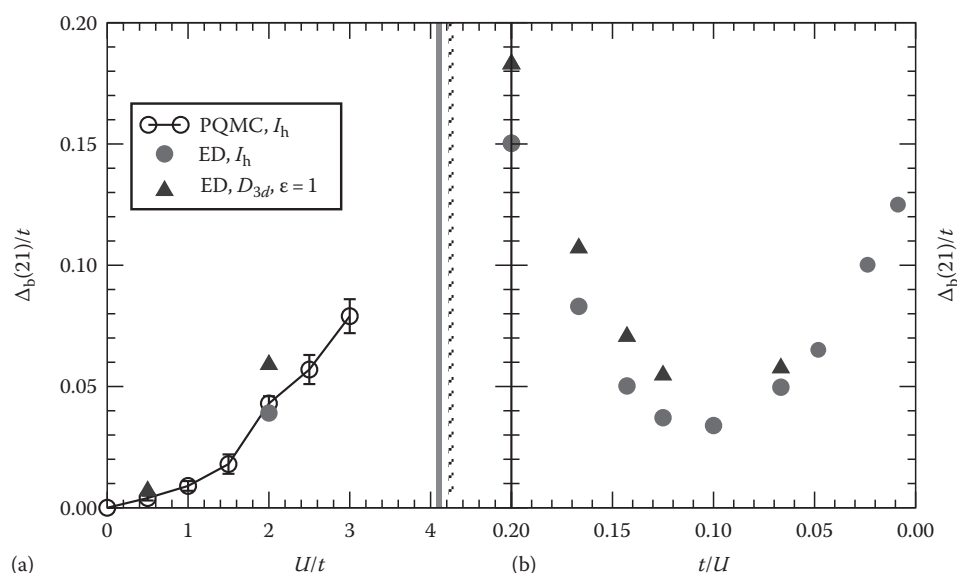


FIGURE 29.5 Schematic illustration of pair-binding energy. Big empty circles represent neutral C₂₀ cage. Small solid dots represent doped electrons.



AQ4 **FIGURE 29.6** Electronic pair-binding energy, $\Delta_b(21)/t$, as a function of U/t . ED (●) and QMC (○) results for the molecule with I_h symmetry. ED results (blue triangle) for the molecule with D_{3d} symmetry. The solid (crossed) vertical line indicates the critical value U_c/t for neutral $I_h(D_{3d})$ molecules. (a) Δ_b versus U/t for $U/t \leq 5$. (b) Δ_b versus t/U for $5 \leq U/t \leq 100$. (Reprinted from Lin, F. et al., *Phys. Rev. B*, 76, 033414, 2007; *J. Phys. Condens. Matter*, 19, 456206, 2007.)

29.3.5.4 Suppression of Jahn–Teller Distortion

Strong electron–electron interactions can also suppress a Jahn–Teller distortion. Figure 29.7 shows the energy difference between a Jahn–Teller distorted and a non-distorted dodecahedral neutral molecule as a function of distortion magnitude, ϵ . We see that, for the stronger electron–electron interaction, $U/t = 8$, which stabilizes a singlet ground state (compared with $U/t = 2$ for which the ground state is a triplet), the effect of the Jahn–Teller distortion is minimal. Taking into account the high ratio, $U/t \sim 7.1$, for the real molecule, we suggest that Jahn–Teller distortion is inactive in the C_{20} fullerene.

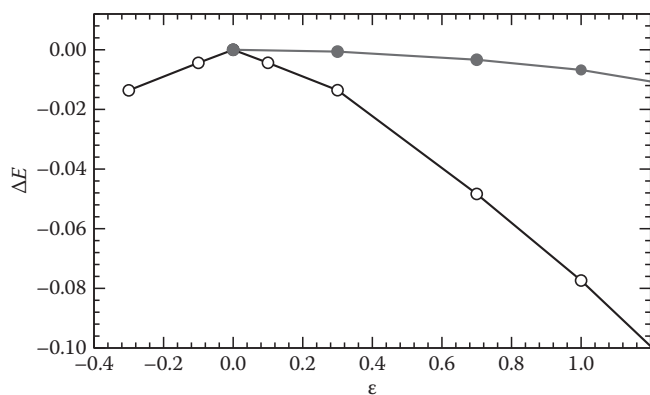


FIGURE 29.7 Shift in the ground state energy of the neutral molecule, ΔE , versus the distortion, ϵ . The Jahn–Teller effect is quite pronounced for $U/t = 2$ (○), but it is essentially absent for $U/t = 8$ (●). (Reprinted from Lin, F. et al., *Phys. Rev. B*, 76, 033414, 2007; *J. Phys. Condens. Matter*, 19, 456206, 2007. With permission.)

29.3.6 Vibration Frequencies and Electron–Phonon Coupling

It has long been conjectured that smaller fullerene molecules, such as C_{20} , will have higher vibration frequencies and larger electron–phonon coupling strength than C_{60} . An approximate equation for the electron–phonon coupling strength is given by $\sim 1800/N_\pi$ meV for aromatic molecules, including fullerene molecules, from tight-binding calculations using the Einstein approximation for phonon frequencies (Devos and Lannoo 1998). Since N_π is the number of electrons in p_π orbitals, C_{20} has the largest electron–phonon coupling strength in the fullerene family, see Figure 29.8. More sophisticated numerical simulations confirm to some extent this trend in the fullerene molecules (Raghavachari et al. 1993, Wang et al. 1996, Saito and Miyamoto 2002). These calculations, though using different equilibrium geometries, show that the C_{20} cage has vibration frequencies approximately in the range of $150 \sim 2200$ cm^{-1} . These vibrational frequencies await a comparison with future Raman scattering and infrared spectroscopy data.

29.4 Solid Properties

So far we have discussed many interesting properties of a single C_{20} fullerene molecule in the above discussions. However, from a practical point of view, the realization of the solid phase of C_{20} fullerene is even more interesting in terms of a possible superconductor or as the building block for the fabrication of nanodevices. Two experimental groups have reported successful syntheses of solid phases of C_{20} fullerenes (Wang et al. 2001, Iqbal et al. 2003). Wang et al. used an ion beam irradiation

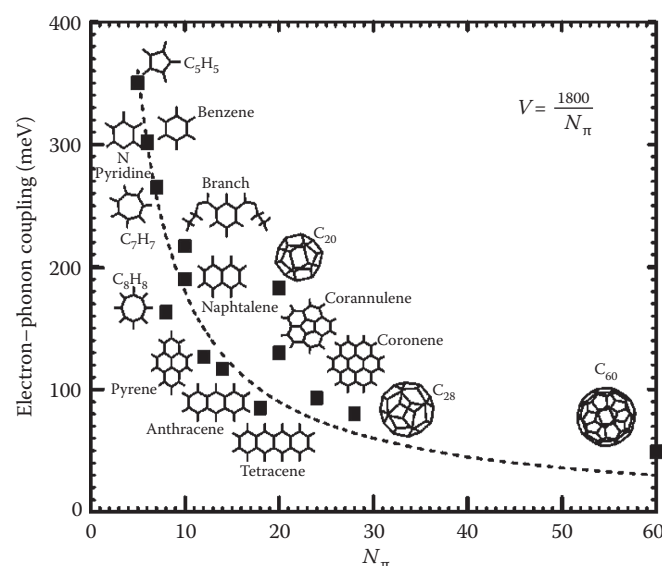


FIGURE 29.8 Dependence of the full electron–phonon coupling, V , on the number of electrons in the p_x molecular orbital. (Reprinted from Devos, A. and Lannoo, M., *Phys. Rev. B*, 58, 8236, 1998. With permission.)

method to produce a hexagonal close-packed crystal, which has a lattice spacing of 4.6 Å, while Iqbal et al. used laser ablation to deposit C₂₀ fullerene molecules into an fcc lattice with fullerene molecules interconnected by two additional carbon atoms per unit cell in the interstitial tetrahedral sites, which is consistent with their DFT calculations. In the following, we shall review work that has been done on solid C₂₀ fullerene, with an emphasis on possible superconductivity in the bulk material. We will also discuss some work on I – V characteristic calculations for a chain constructed from C₂₀ fullerene molecules, which may be important for the future development of fullerene-based nanodevices.

29.4.1 Superconductivity?

The fact that both superconducting alkali-metal-doped C₆₀ solid and the pure C₂₀ solid have an fcc lattice structure has led Spagnolatti et al. to speculate about doping one Na atom per unit cell in the remaining empty octahedral site in a C₂₀ fcc solid (Spagnolatti et al. 2002) (In fcc solid C₆₀, both the octahedral site and the two tetrahedral sites are occupied by three K atoms, leading to the chemical configuration of K₃ C₆₀ in the superconducting phase). The undoped solid is an insulator with a band gap of 2.47 eV. With Na doping, the energy bands still look like the pure solid case, and the doping shifts the Fermi energy into the lowest conduction bands. Hence, the solid turns from an undoped insulator into a metal. See Figure 29.9 for the fcc lattice structure and Figure 29.10 for the density of states (DOS) of the Na-doped C₂₂ fcc solid. The electron–phonon coupling strength, λ , is also calculated to be $\lambda = 1.12$, much larger than the value for the solid C₆₀ where $\lambda \sim 0.3 - 0.5$ (Gunnarsson 2004). Using McMillan’s formula, which is valid for phonon-mediated superconductivity, Spagnolatti et al. then estimated the superconducting transition

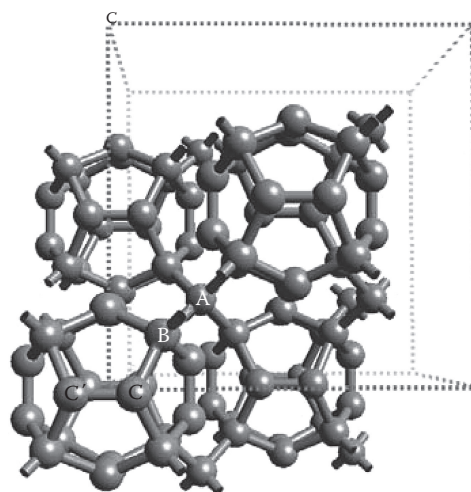


FIGURE 29.9 The fcc lattice structure of the C₂₂ crystal. The lattice constant is 8.61 Å. The coordinates of the three independent atoms A, B, and C are given by, in units of lattice constant, $A = (0.25, 0.25, 0.25)$, $B = (0.148, -0.148, 0.148)$, and $C = (0.078, -0.217, 0.0)$. Eight atoms out of the twenty of the cage (B) and the interstitial carbon atoms (A) are sp^3 hybridized. The other twelve atoms of the cage (C) are sp^2 hybridized. In the NaC₂₂ compound, the alkali atoms occupy the octahedral site of the fcc lattice. (Reprinted from Spagnolatti, I. et al., *Europhys. Lett.*, 59, 572, 2002. With permission.)

temperature to be in the range of 15–55 K, an impressive range for phonon-mediated superconductivity.

An earlier theoretical speculation on the possible forms of solid C₂₀ phase using DFT calculations has predicted the simple cubic (SC) lattice to be the most stable one, and this structure has the property of being metallic (Miyamoto and Saito, 2001). However, the C₂₀ cage structure must be broken in order to form such a SC lattice, which reduces the electron–phonon coupling strength and hence is not likely to produce a high transition temperature for superconductivity even if such a lattice could superconduct. They also suggest that a one-dimensional chain of C₂₀ cages can have a higher transition temperature if it is doped with either electrons or holes to shift the Fermi level to the peak of the DOS. As promising as this may seem, there is no experimental realization of such lattices up to now. Furthermore, DFT investigations (Okada et al. 2001) show that orthorhombic and tetragonal lattices with the polymerized C₂₀ cage as a building block have much lower energies than the SC lattice. Calculations of DOS suggest that both lattices are semiconductors with energy gaps of 1.4 and 1.7 eV for orthorhombic and tetragonal lattices, respectively. Their DOS figures also show that, with slight hole doping, the Fermi level can be moved to the peaks of the valence bands, hence making them possible candidates for superconductors. Polarization and dielectric constants of orthorhombic and tetragonal lattices have also been studied by DFT (Otsuka et al. 2006). The dielectric constants are rather anisotropic and assume values in the range of 4.7 ~ 5.8 depending on the direction of the applied external electric field.

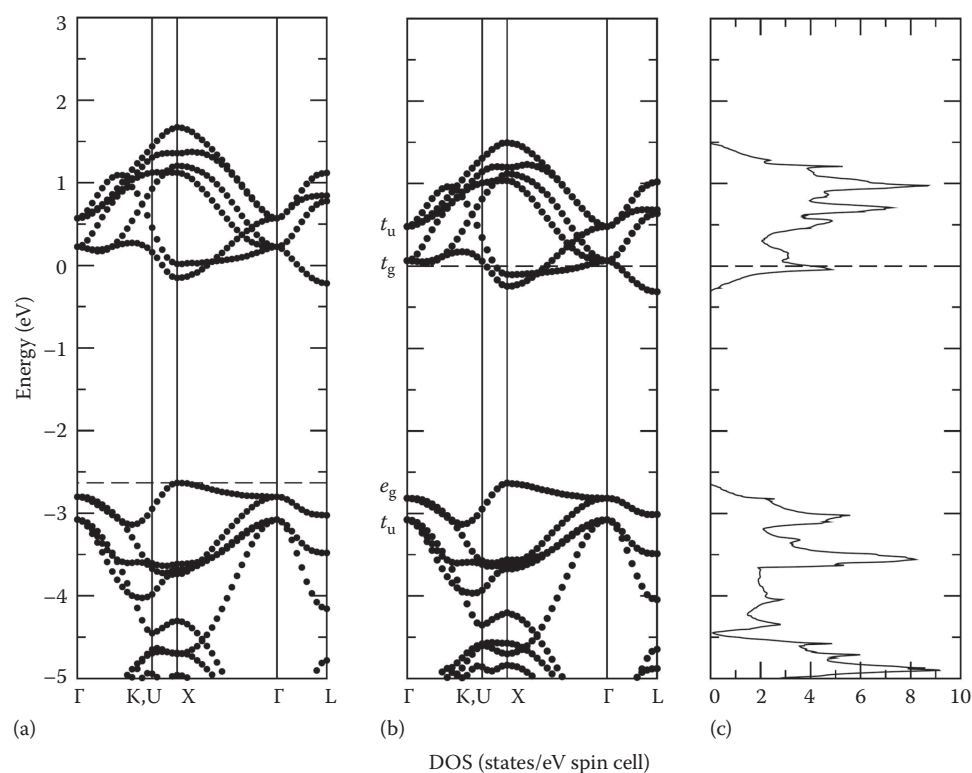


FIGURE 29.10 Band structure around the Fermi level of (a) the pure fcc C_{22} and (b) NaC_{22} crystals. The zero of the energy is the Fermi level of NaC_{22} . The DOS of NaC_{22} is shown in (c). (Reprinted from Spagnolatti, I. et al., *Europhys. Lett.*, 59, 572, 2002. With permission.)

As discussed in the pair-binding energy calculation in the above section, purely electronic correlations have been argued to be responsible for the superconductivity in alkali-metal-doped C_{60} solid (Chakravarty et al. 1991). In this mechanism, doped electrons pair up and lead to superconductivity inside one molecule. The Josephson coupling between superconducting molecules then makes the supercurrent flow without resistance in the whole solid. ED and QMC calculations on a Hubbard C_{20} molecule show, however, that the pair-binding energy does not favor such a mechanism (Lin et al. 2007). But this calculation does show a metal-insulator transition as a function of the interaction strength, U/t , see Figure 29.11. For the value of $U/t \sim 7.1$ for the real material, undoped C_{22} in an fcc lattice is insulating, in agreement with the DFT prediction (Spagnolatti et al. 2002).

29.4.2 I - V Characteristics of Cage Chains

We have seen experimental evidence that the synthesis of solid fcc C_{20} is a candidate for a possible new superconductor. However, there is another application direction for fullerene molecules, that is, fabrication of nanometer electro-mechanical systems (NEMS) for use in circuits at the nanometer scale. For this purpose, it is important to understand the electronic properties of such a device, especially the I - V characteristics of nanodevices made of C_{20} cages. As already discussed by Miyamoto and Saito (2001), 1D double or single-bonded C_{20} chains are semiconductors, implying a possible application in nanocircuits. We will

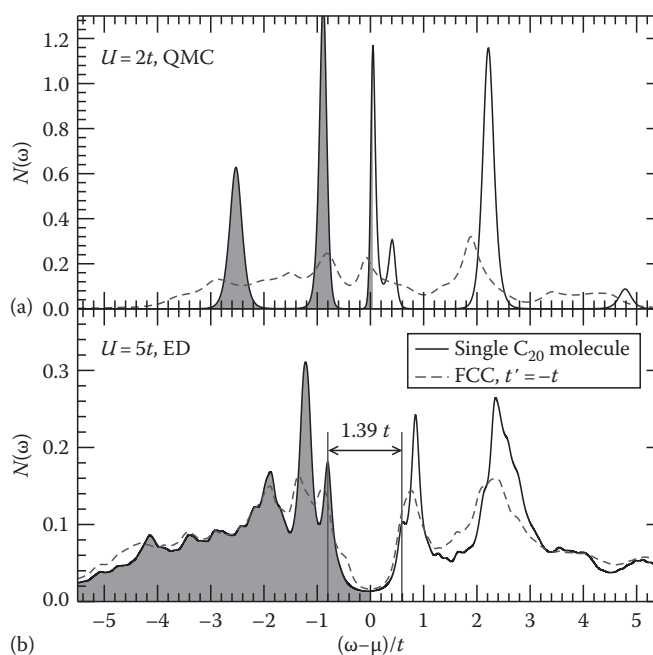


FIGURE 29.11 DOS $N(\omega)$ at (a) $U = 2t$ from QMC and at (b) $U = 5t$ from ED. In both panels, the DOS for the C_{22} fcc lattice obtained from CPT with $t' = -t$ is shown as a dashed line. (Reprinted from Lin, F. et al., *Phys. Rev. B*, 76, 033414, 2007; *J. Phys. Condens. Matter*, 19, 456206, 2007. With permission.)

concentrate on transport properties of 1D C₂₀ chains, specifically on theoretical calculations of the electrical conductivity of C₂₀ monomers, dimers, and longer chains, embedded between two electrodes or molecular interfaces (Roland et al. 2001, Otani et al. 2004, Ouyang and Xu 2007).

DFT calculations together with the Keldysh nonequilibrium Green's functions formalism (Datta 1995) allow one to calculate the *I-V* curve from first principles. Applications of such techniques to short chains of C₂₀ with different geometries show that, for multi-bonded short C₂₀ chains between Al(100) leads, the electrical conductivity has little dependence on the number of C₂₀ molecules in between (Roland et al. 2001); for double- and single-bonded short chains between Au jellium electrodes, the electrical conductivity depends strongly on the number of C₂₀ molecules in between, i.e., a monomer has an electrical conductivity that is about one order of magnitude greater than the dimer (Otani et al. 2004). For multi- and double-bonded short chains between two single-wall carbon nanotube electrodes, the electrical conductivity again strongly depends on the number of C₂₀ molecules in between, with monomers having significantly larger conductivity than dimers (Ouyang and Xu 2007). It is also worth noting that, by replacing one C atom with one N atom per C₂₀ molecule, the electrical conductivity increases substantially (Ouyang and Xu 2007). The effect of molecular vibrations on the *I-V* characteristics of a C₂₀ fullerene bridge between two gold electrodes has also been studied by TBMD, which shows large discontinuous steps in the differential conductance at vibration frequencies of the molecule (Yamamoto et al. 2005).

To summarize, the above several calculations suggest some features for the short chains of C₂₀ cages: (1) The connection between the electrodes and the C₂₀ molecule is important for electron transport through the chains; (2) Electron scattering at C₂₀-C₂₀ junctions greatly reduces the conductivity; (3) Doping can significantly change the electrical conductivity; (4) Molecular vibrations greatly affect electron transport. However, in the above calculations an exact treatment of strong electron correlations is still missing. Its effect on the electron transport properties of short C₂₀ chains still needs to be calculated.

29.5 Summary and Future Perspective

We have given a survey of both single molecular and possible solid-state properties of C₂₀ fullerenes. DFT and other mean-field calculations give conflicting ground state energy orderings for C₂₀ isomers, but this situation is resolved by more accurate QMC simulations. This demonstrates the need to take into account electron correlations in predicting the C₂₀ fullerene electronic properties. By fitting parameters in an effective one-band Hubbard model defined on a C₂₀ fullerene, it has been possible to demonstrate the effect of strong electron correlations: magnetic to nonmagnetic molecule transition, metal to insulator transitions, and the suppression of Jahn-Teller distortion, all of which are driven by strong electron interactions. As to the examination of possible superconducting properties that has stimulated most of the theoretical and experimental endeavors discussed

in this chapter, we feel it is necessary to take into account both the strong electronic correlations and the equally important electron-phonon coupling. A balanced treatment of both interactions together with an exact calculation seems to be a challenging but worthwhile problem in the field. On the experimental side, it is really important to synthesize larger quantities of solid C₂₀. Larger and better samples will allow theoretical calculations to be tested experimentally. To summarize, we have seen in this chapter many interesting properties of the C₂₀ fullerene, the smallest and truly unique member of the fullerene family.

Acknowledgments

FL is supported by the US Department of Energy under award number DE-FG52-06NA26170. ESS, CK, and AJB are supported by the Natural Sciences and Engineering Research Council of Canada and the Canadian Foundation for Innovation. CK and AJB are supported by the Canadian Institute for Advanced Research.

References

- Allison, C. and K. A. Beran, Energetic analysis of 24 C₂₀ isomers, *J. Mol. Struct. (Theochem)* **680**, 59 (2004).
- An, W., Y. Gao, S. Bulusu, and X. C. Zeng, Ab initio calculation of bowl, cage, and ring isomers of C₂₀ and C₂₀⁻, *J. Chem. Phys.* **122**, 204109 (2005).
- Barnett, R. N., P. J. Reynolds, and W. A. Lester Jr., Electron affinity of fluorine: A quantum Monte Carlo study, *J. Chem. Phys.* **84**, 4992 (1986).
- Brabec, C. J., E. B. Anderson, B. N. Davidson et al., Precursors to C₆₀ fullerene formation, *Phys. Rev. B* **46**, 7326 (1992).
- Cao, Z. X., Electronic structure and stability of C₂₀ isomers, *Chin. Phys. Lett.* **18**, 1060 (2001).
- Chakravarty, S., M. P. Gelfand, and S. Kivelson, Electronic correlation effects and superconductivity in doped fullerenes, *Science* **254**, 970 (1991).
- Collins, P. G., J. C. Grossman, M. Côté et al., Scanning tunneling spectroscopy of C₃₆, *Phys. Rev. Lett.* **82**, 165 (1999).
- Datta, S. *Electronic Transport in Mesoscopic Systems*. New York: Cambridge University Press (1995).
- Davydov, I. V., A. I. Podlivaev, and L. A. Openov, Anomalous thermal stability of metastable C₂₀ fullerene, *Phys. Solid State* **47**, 778 (2005).
- Devos, A. and M. Lannoo, Electron-phonon coupling for aromatic molecular crystals: Possible consequences for their superconductivity, *Phys. Rev. B* **58**, 8236 (1998).
- Du, A. J., Z. Y. Pan, Y. K. Ho, Z. Huang, and Z. X. Zhang, Memory effect in the deposition of C₂₀ fullerenes on a diamond surface, *Phys. Rev. B* **66**, 035405 (2002).
- Ehlich, R., P. Landenberger, and H. Prinzbach, Coalescence of C₂₀ fullerenes, *J. Chem. Phys.* **115**, 5830 (2001).
- Ellzey, M. L. Jr., Finite group theory for large systems. I. Symmetry-adaptation, *J. Chem. Inf. Comput. Sci.* **43**, 178 (2003).

- Ellzey, M. L. Jr., Finite group theory for large systems. 3. Symmetry-generation of reduced matrix elements for icosahedral C_{20} and C_{60} molecules, *J. Comput. Chem.* **28**, 811 (2007).
- Ellzey, M. L. Jr. and D. Villagran, Finite group theory for large systems. 2. Generating relations and irreducible representations for the icosahedral point group, *J. Chem. Inf. Comput. Sci.* **43**, 1763 (2003).
- Feyereisen, M., M. Gutowski, J. Simons, and J. Almlöf, Relative stabilities of fullerene, cumulene, and polyacetylene structures for C_n ; $n = 18-60$, *J. Chem. Phys.* **96**, 2926 (1992).
- Grossman, J. C., L. Mitas, and K. Raghavachari, Structure and stability of molecular carbon: Importance of electron correlation, *Phys. Rev. Lett.* **75**, 3870 (1995).
- Gunnarsson, O. *Alkali-Doped Fullerenes: Narrow-Band Solids with Unusual Properties*. Singapore: World Scientific Publishing (2004).
- Harrison, W. A. *Electronic Structure and the Properties of Solids: The Physics of the Chemical Bond*. New York: Dover Publication (1989).
- Hebard, A. F., M. J. Rosseinsky, R. C. Haddon et al., Superconductivity at 18 K in potassium-doped C_{60} , *Nature* **350**, 600 (1991).
- Iqbal, Z., Y. Zhang, H. Grebel et al., Evidence for a solid phase of dodecahedral C_{20} , *Eur. Phys. J. B* **31**, 509 (2003).
- Ke, X. Z., Z. Y. Zhu, F. S. Zhang, F. Wang, and Z. X. Wang, Molecular dynamics simulation of C_{20} fullerene, *Chem. Phys. Lett.* **313**, 40 (1999).
- Konstantinidis, N. P. Antiferromagnetic Heisenberg model on clusters with icosahedral symmetry, *Phys. Rev. B* **72**, 064453 (2005).
- Konstantinidis, N. P. Unconventional magnetic properties of the icosahedral symmetry antiferromagnetic Heisenberg model, *Phys. Rev. B* **76**, 104434 (2007).
- Kroto, H. W. The stability of the fullerenes C_n , with $n = 24, 28, 32, 36, 50, 60$ and 70 , *Nature* **329**, 529 (1987).
- Kroto, H. W. Symmetry, space, stars and C_{60} , *Rev. Mod. Phys.* **69**, 703 (1997).
- Kroto, H. W., J. R. Heath, S. C. O'Brien, R. F. Curl, and R. E. Smalley, C_{60} : Buckminsterfullerene, *Nature* **318**, 162 (1985).
- Lin, F. and E. S. Sørensen, Estimates of effective Hubbard model parameters for C_{20} isomers, *Phys. Rev. B* **78**, 085435 (2008).
- Lin, F., E. S. Sørensen, C. Kallin, and A. J. Berlinsky, Strong correlation effects in the fullerene C_{20} studied using a one-band Hubbard model, *Phys. Rev. B* **76**, 033414 (2007); Extended Hubbard model on a C_{20} molecule, *J. Phys. Condens. Matter* **19**, 456206 (2007).
- Lindemann, F. The calculation of molecular vibration frequencies, *Z. Phys.* **11**, 609 (1910).
- López-Sandoval, R. and G. M. Pastor, Electron correlations in a C_{20} fullerene cluster: A lattice density-functional study of the Hubbard model, *Eur. Phys. J. D* **38**, 507 (2006).
- Luo, J., L. M. Peng, Z. Q. Xue, and J. L. Wu, Positive electron affinity of fullerenes: Its effect and origin, *J. Chem. Phys.* **120**, 7998 (2004).
- Miyamoto, Y. and M. Saito, Condensed phases of all-pentagon C_{20} cages as possible superconductors, *Phys. Rev. B* **63**, R161401 (2001).
- Okada, S., Y. Miyamoto, and M. Saito, Three-dimensional crystalline carbon: Stable polymers of C_{20} fullerene, *Phys. Rev. B* **64**, 245405 (2001).
- Otani, M., T. Ono, and K. Hirose, First-principles study of electron transport through C_{20} cages, *Phys. Rev. B* **69**, 121408(R) (2004).
- Otsuka, J., T. Ono, K. Inagaki, and K. Hirose, First-principles calculations of dielectric constants of C_{20} bulk using Wannier functions, *Physica B* **376-377**, 320 (2006).
- Ouyang, F. P. and H. Xu, Electronic transport in molecular junction based on C_{20} cages, *Chin. Phys. Lett.* **24**, 1042 (2007).
- Paquette, L. A., R. J. Ternansky, D. W. Balogh, and G. J. Kentgen, Total synthesis of dodecahedrane, *J. Am. Chem. Soc.* **105**, 5446 (1983).
- Parasuk, V. and J. Almlöf, C_{20} : The smallest fullerene? *Chem. Phys. Lett.* **184**, 187 (1991).
- Piskoti, C., J. Yarger, and A. Zettl, C_{36} , a new carbon solid, *Nature* **393**, 771 (1998).
- Prinzbach, H., A. Weller, P. Landenberger et al., Gas-phase production and photoelectron spectroscopy of the smallest fullerene, C_{20} , *Nature* **407**, 60 (2000).
- Raghavachari, K., D. L. Strout, G. K. Odom et al., Isomers of C_{20} : Dramatic effect of gradient corrections in density functional theory, *Chem. Phys. Lett.* **214**, 357 (1993).
- Roland, C., B. Larade, J. Taylor, and H. Guo, Ab initio I-V characteristics of short C_{20} chains, *Phys. Rev. B* **65**, 041401(R) (2001).
- Saito, M. and Y. Miyamoto, Vibration and vibronic coupling of C_{20} isomers: Ring, bowl, and cage clusters, *Phys. Rev. B* **65**, 165434 (2002).
- Schmalz, T. G., W. A. Seitz, D. J. Klein, and G. E. Hite, C_{60} carbon cages, *J. Am. Chem. Soc.* **110**, 1113 (1988).
- Sokolova, S., A. Lüchow, and J. B. Anderson, Energetics of carbon clusters C_{20} from all-electron quantum Monte Carlo calculations, *Chem. Phys. Lett.* **323**, 229 (2000).
- Spagnolatti, I., M. Bernasconi, and G. Benedek, Electron-phonon interaction in the solid form of the smallest fullerene C_{20} , *Europhys. Lett.* **59**, 572 (2002).
- Taylor, P. R., E. Bylaska, J. H. Weare, and R. Kawai, C_{20} : Fullerene, bowl or ring? New results from coupled-cluster calculations, *Chem. Phys. Lett.* **235**, 558 (1995).
- Ternansky, R. J., D. W. Balogh, and L. A. Paquette, Dodecahedrane, *J. Am. Chem. Soc.* **104**, 4503 (1982).
- Wang, L. S., J. Conceicao, C. M. Jin, and R. E. Smalley, Threshold photodetachment of cold C_{60}^- , *Chem. Phys. Lett.* **182**, 5 (1991).
- Wang, Z., P. Day, and R. Pachter, Ab initio study of C_{20} isomers: Geometry and vibrational frequencies, *Chem. Phys. Lett.* **248**, 121 (1996).
- Wang, X. B., C. F. Ding, and L. S. Wang, High resolution photoelectron spectroscopy of C_{60} , *J. Chem. Phys.* **110**, 8217 (1999).

- Wang, Z., X. Ke, Z. Zhu et al., A new carbon solid made of the world's smallest caged fullerene C₂₀, *Phys. Lett. A* **280**, 351 (2001).
- Wang, C. R., Z. Q. Shi, L. J. Wan et al., C₆₄H₄: Production, isolation, and structural characterizations of a stable unconventional fulleride, *J. Am. Chem. Soc.* **128**, 6605 (2006).
- Xie, S. Y., F. Gao, X. Lu et al., Capturing the labile fullerene[50] as C₅₀Cl₁₀, *Science* **304**, 699 (2004).
- Xu, S. H., M. Y. Zhang, Y. Y. Zhao, B. G. Chen, J. Zhang, and C. C. Sun, Super-valence phenomenon of carbon atoms in C₂₀ molecule, *J. Mol. Struct. (Theochem)* **760**, 87 (2006).
- Yamamoto, T., K. Watanabe, and S. Watanabe, Electronic transport in fullerene C₂₀ bridge assisted by molecular vibrations, *Phys. Rev. Lett.* **95**, 065501 (2005).
- Yang, S. H., C. L. Pettiette, J. Conceicao, O. Cheshnovsky, and R. E. Smalley, UPS of Buckminsterfullerene and other large clusters of carbon, *Chem. Phys. Lett.* **139**, 233 (1987).

Author Queries

[AQ1] Please check the inserted year for Ellzey (2003).

[AQ2] The value 3370 K is given as 3372 K in artwork of Figure 29.4. Please check.

[AQ3] Please check whether "AFM" should be changed to "AHM"

[AQ4] In the caption of Figure 29.6, "molecular with I_h symmetry" has been changed to "molecule with I_h symmetry". Please check.

Also provide an alternative description for "blue triangle" as this figure is to be set in grayscale.

[AQ5] Please check the inserted year for Kroto (1987).

